# Kinetics of precipitation in Al–1 wt% Mn alloy

A. K. JENA, D. P. LAHIRI, T. R. RAMACHANDRAN
*Department of Metallurgical Engineering, Indian Institute of Technology, Kanpur, India*

M. C. CHATURVEDI
*Department of Mechanical Engineering, University of Manitoba, Winnipeg, R3T 2N2, Canada*

Precipitation kinetics in high purity Al–10 wt% Mn alloy has been investigated during the early stages of isothermal annealing between 823 and 698 K by resistivity measurements. Aged specimens were also examined by transmission electron microscopy. The precipitation kinetics can be represented by an Avrami type equation with the time exponent $n = 2/3$ during the early stages of annealing. This can be attributed to the nucleation and growth of flat needle-like precipitates on dislocations. The precipitates were $Al_6Mn$ at $\geqslant 773$ K and the metastable $G_2$-phase at $\leqslant 773$ K. After prolonged annealing times at 848 K, isometric plates of $Al_6Mn$ were also observed and the value of $n$ was found to be 1.0. However, at 698 K after longer annealing times, isometric needles of $Al_{12}Mn$, G-phase were observed along with flat needles of $G_2$ precipitate. At 698 K, the value of $n$ tends to decrease with time from 0.67 to 0.59.

## 1. Introduction

In aluminium, the maximum solubility of manganese is 2.0 wt% at the eutectic temperature of 958.5 K and decreases rapidly with a decrease in temperature [1]. The decomposition kinetics of Al–Mn alloys containing about 1.0% Mn have been examined by several investigators using resistivity measurements [2–4]. The results of these investigations, however, are not in complete agreement. This, in part, may be attributed to the presence of impurities since small amounts of iron (0.01 wt%) and other elements are known to change the decomposition behaviour appreciably [3, 5, 6].

In Al–Mn alloys, the equilibrium phase $Al_6Mn$ with an orthorhombic structure [7] is reported to be the main precipitating phase above 798 K with a metastable G-phase precipitating below 823 K [3, 8]. Using X-ray [9, 10] and electron diffraction [3, 5, 11] the structure of this phase has been established as bcc with a lattice parameter of 7.48 to 7.58 Å. The existence of a second metastable phase of unknown structure has been reported by Oetschägel et. al. [2, 11]. Goel and co-workers [3] have also observed a metastable phase with a structure similar to that of $Al_{24}Mn_5Zn$ [12]. The morphologies of these phases as a function of aging temperature and the kinetics of precipitation in the early stages have not been investigated. In the present investigation, the decomposition behaviour of a high purity Al–1 wt% Mn alloy, particularly in the early stages of aging, has been examined by resistivity measurements. The resistivity results have been supplemented by structural data obtained from transmission electron microscopy.

## 2. Experimental techniques

The Al–Mn alloys were prepared by melting aluminium (99.999%) and manganese (99.999%) in a vacuum induction furnace under an argon atmosphere. The alloys were homogenized at 898 K for 4 days, swaged and drawn into 0.9 mm wires for the resistivity measurements or rolled into 0.20 mm thick strips for electron microscopy. The composition of the alloys was determined
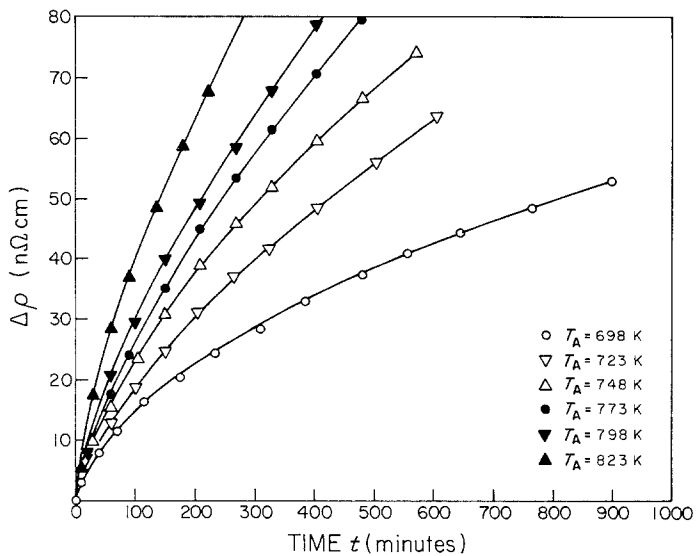
by spectroscopic analysis. The alloy used for precipitation studies contained 1.00 wt% Mn with Mg and Cu content less than 0.001 wt%. Two other alloys used for resistivity measurements contained 0.1 and 0.35 wt% Mn with Si, Cu and Ti content less than 0.001 wt%.

All the specimens were solution treated and aged in air furnaces with the temperature controlled to ± 1 K. The resistivities of the heat treated wire specimens were measured at liquid nitrogen temperature (78 K) by using a precision Leeds and Northrup Kelvin bridge. By suitably adjusting the length to diameter ratio of the specimens, it was possible to detect a change in resistivity of $\sim 10^{-10}$ $\Omega$ cm. Thin foils for electron microscopy were prepared by jet electropolishing 3 mm discs in a 5% perchloric acid—methanol bath at 250 K and 15 V. They were examined in a Philips 300 electron microscope.

## 3. Results
### 3.1. Resistivities of homogeneous alloys
The wire specimens of 99.999% Al and its alloys containing 0.1, 0.35 and 1.0 wt% Mn were annealed for 3 h at 893 K and air cooled. Air cooling is considered adequate to remove thermal vacancies and prevent the precipitation reaction [13]. The resistivities of these samples measured at 73 and 297 K are given by

$$\rho_{78} = 0.24 + 7.10\,x \qquad (1)$$

$$\rho_{293} = 2.65 + 6.50\,x \qquad (2)$$

where $\rho$ is the resistivity in $\mu\,\Omega$ cm and $x$ is the

manganese content in at%. The observed values of the resistivity of pure aluminium and its composition dependence are in good agreement with the reported values of 0.23 $\mu\,\Omega$ cm for resistivity [14] and 6.9 [15] and 7.6 [16] for the Mn composition dependence at 78 K.

### 3.2. Resistivity changes during isothermal annealing
Homogenized wire specimens of Al—1.0 wt% Mn alloy were soaked for 15 min at 893 K, quenched in iced $CaCl_2$ solution at 271 K and isochronally annealed for 15 min at each one of a series of successively increasing temperatures. Resistivity changes during isochronal annealing suggest that the precipitation reaction starts above 573 K [13]. Oelschlägel *et al.* [2, 11] however, have reported that observable changes in the resistivity of a high purity Al—1.2 wt% Mn alloy occur above 723 K.

The resistivity of a quenched specimen annealed for 10 min at 273 K and a further 10 min at 573 K was taken as the reference resistivity, $\rho_0$. The specimen was then isothermally annealed at a fixed temperature and the resistivity $\rho_t$ measured as a function of time, $t$. The isothermal annealing experiments were performed at 698, 723, 748, 773, 798 and 823 K for a period of 6 to 15 h. The results are shown in Fig. 1 as plots of $\Delta\rho = (\rho_0 - \rho_t)$ against time, $t$. It is seen that at each annealing temperature $\Delta\rho$ increases with a decreasing rate and the rate of increase increases with temperature.

Another specimen of Al—1.0 wt% Mn alloy was solution treated, quenched from 893 K and isothermally annealed at 848 K. The resistivity was
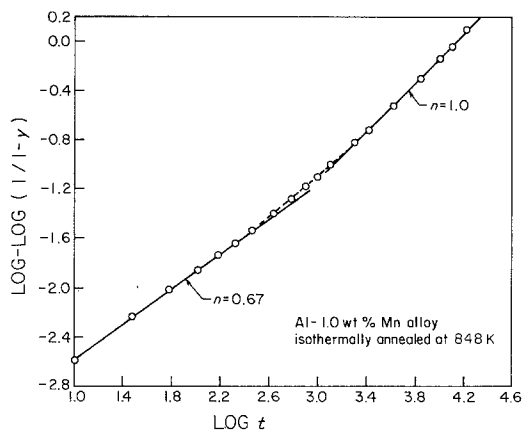
*Figure 2* Log–log plot of log $1/(1 - Y)$ against $t$ at 848 K.

monitored for more than 376 h until its value remained constant with time at $2.75 \times 10^{-6}\, \Omega\,\text{cm}$. From Equation 1 the solubility of Mn in aluminium at 848 K was calculated to be 0.71 wt% which is in good agreement with that given in the literature [1]. It was therefore concluded that the precipitation reaction was complete and the final resistivity was taken as the resistivity after an infinite time of annealing, $\rho_\infty$. Equation 1 shows that the resistivity of an alloy is linearly related to its average solute content $\bar{C}$. Therefore,

$$\frac{\Delta\rho}{\Delta\rho_\infty} = \frac{\rho_0 - \rho_t}{\rho_0 - \rho_\infty} = \frac{\bar{C}_{t=0} - \bar{C}_t}{\bar{C}_{t=0} - \bar{C}_{t-\infty}} = Y \quad (3)$$

where $Y$ denotes fraction transformed. The isothermal annealing data obtained at 848 K are converted into $Y$ via Equation 3 and shown in the usual plot of log log $[1/(1 - Y)]$ against log $t$ in Fig. 2. Two linear parts of the curve with slopes of 0.67 and 1.0 are distinguishable.

## 3.3. Structural examination

0.2 mm strip specimens were given a final solution treatment at 893 K for 20 min and air cooled. They were then annealed at 848, 823, 773, 723 and 698 K for various lengths of time. Both solution treated and aged samples were examined by transmission electron microscopy. The solution treated specimens were observed to be free from vacancy loops as well as precipitates.

Thin plates of $Al_6Mn$ phase with one dimension much longer than the others were observed in specimens aged for 97 min at 848 K, 310 and 1544 min at 823 K and 680 and 5790 min at 773 K. A typical example of $Al_6Mn$ phase of this morphology is shown in Fig. 3a which is the structure of a specimen aged for 310 min at 823 K. The selected area diffraction pattern of $Al_6Mn$ precipitate is shown in Fig. 3b. The orientations of the matrix and precipitate are $[0\,1\,3]$ and $[1\,\bar{2}\,1]$, respectively. In specimens aged for longer times in the 773 to 848 K temperature region, $Al_6Mn$ plates of a different morphology, i.e. with length and width of comparable dimensions, were also observed. Fig. 4a shows an example of $Al_6Mn$ precipitate plate of such a shape observed in a specimen aged for 5790 min at 773 K. The selected area diffraction pattern of the precipitate is shown in Fig. 4b. The matrix is in the $[1\,1\,0]$ orientation and the precipitate can only be indexed as $Al_6Mn$ with the $[0\,\bar{2}\,1]$ axis parallel to the electron beam. A definite orientation relationship between $Al_6Mn$ plates and the matrix could not be established, but most of them were observed to lie on $\{0\,1\,1\}$ type matrix planes.

At aging temperatures of $\leqslant 773$ K and upon longer aging times, a metastable phase $Al_{12}Mn$,
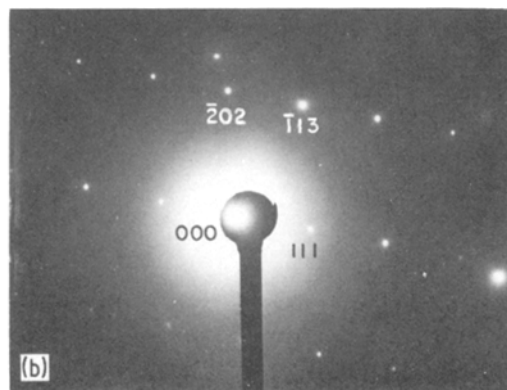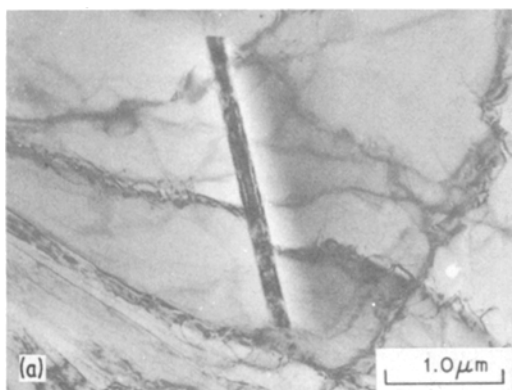


*Figure 3* (a) Flat needle shape $Al_6Mn$ precipitate in a specimen aged for 310 min at 823 K, (b) selected area diffraction pattern from the precipitate shown in Fig. 3a: Matrix $[0\,1\,3]$; precipitate $[1\,\bar{2}\,1]$.
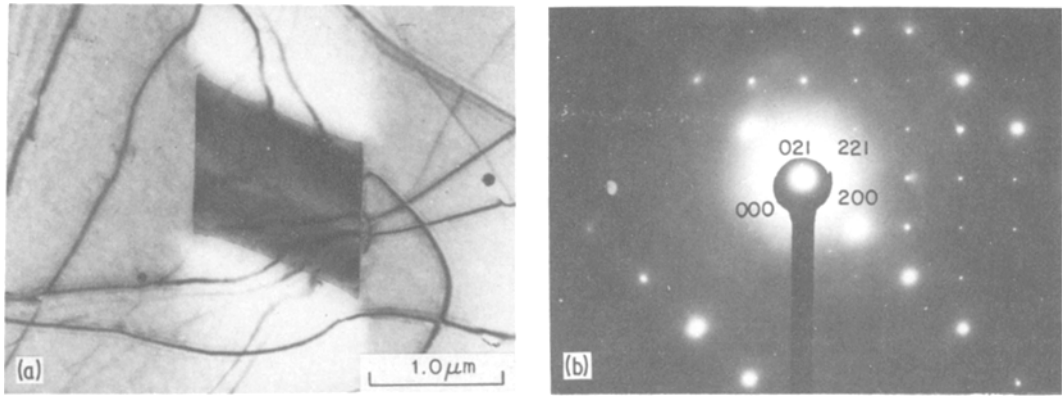
Figure 4 (a) $Al_6Mn$ precipitate in a specimen aged for 5790 min at 773 K, (b) selected area diffraction pattern of precipitate shown in Fig. 4a: Matrix [110]; precipitate[0$\bar{1}$2].

also known as phase G, with a bcc structure was observed. An example of this phase in a specimen aged for 5790 min at 773 K is shown in Fig. 5a with its diffraction pattern in Fig. 5b. The (310) plane of this phase is observed to be parallel to the (111) plane of the aluminium matrix which is similar to that reported earlier [5]. The lattice parameter of this phase determined by electron diffraction was found to be 7.55 Å which is also in agreement with the values reported by other investigators.

In specimens aged at 773 K and lower temperatures, another metastable phase $G_2$ was observed. This was found to be similar to the one reported by Goel *et. al.* [3], i.e. orthorhombic structure with lattice parameters, $a = 25$ Å, $b = 24.8$ Å and $c = 30.3$ Å. The shape of this precipitate was a flat needle as shown in Fig. 6a which is the structure of a specimen aged for 5790 min at 773 K. The diffraction pattern of the precipitate is reproduced in Fig. 6b. These precipitates did not show a unique orientation relationship with the matrix but the majority of them were observed to lie on {011} type aluminium planes and their growth direction was parallel to either the ⟨111⟩ or ⟨100⟩ aluminium directions.

In the specimen aged for 740 min at 723 K, only a few precipitates on or near dislocations were observed as shown in Fig. 7. These precipitates did not give rise to a diffraction pattern and therefore could not be identified. At 698 K, however, after a similar aging time, no precipitate particles were detected.

## 4. Discussion

The extent of a precipitation reaction as a function of time can in general be expressed by an equation of the following type [17]

$$Y = 1 - \exp(-kt^n) \tag{4}$$



Figure 5 (a) Flat needle shape G-phase in a specimen aged for 5790 min at 773 K, (b) selected area diffraction pattern of precipitate shown in Fig. 5a: Matrix [110]; precipitate [023].
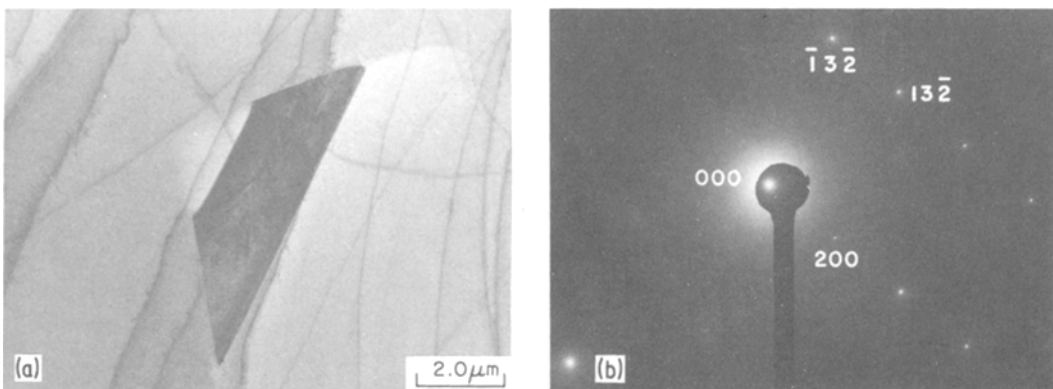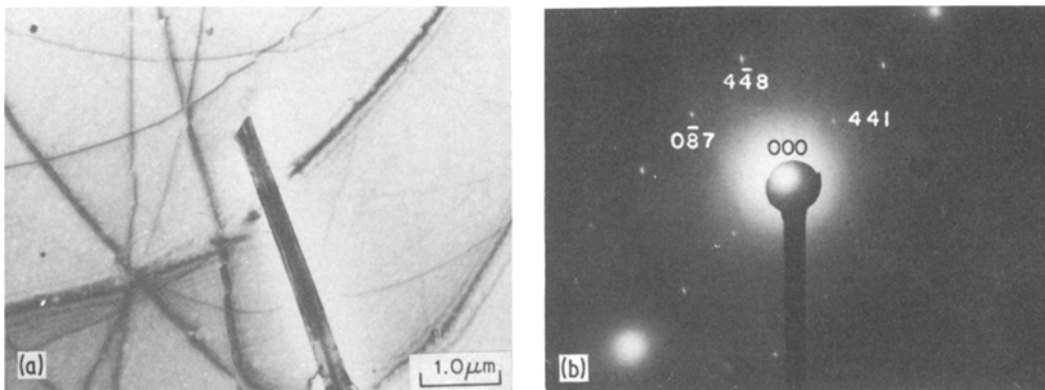
2547

Figure 6 (a) Flat needle shape $G_2$-phase in a specimen aged for 5790 min at 773 K, (b) selected area diffraction pattern of precipitate shown in Fig. 6a: Matrix [110]; precipitate [9$\bar{7}$8].

where $k$ and $n$ are constants. $k$ is a rate constant determined by the chemistry of the precipitate and the activation energy required for nucleation and growth. The coefficient $n$ is determined by the time dependence of the nucleation rate and the growth rates of various dimensions of the precipitate. Thus morphology and the distribution of the precipitate determine $n$. It follows from Equation 4 that the slope of the log log [1/(1 − $Y$)] against log $t$ plot is $n$. Fig. 2 shows that the value of $n$ changes from $n = 0.67$ at $t < 300$ min to $n = 1.0$ at $t > 2300$ min for the Al−1 wt% Mn alloy annealed at 848 K. The isothermal annealing data obtained at lower temperatures (Fig. 1) cannot be treated in this manner as the value of $\Delta\rho_\infty$ at those temperatures is not known. However, the amount of precipitation at the end of annealing at these temperatures is low. For example, at 773 K the solubility of Mn in Al is 0.3 wt% [1]. Hence, from Equation 1 $\Delta\rho_\infty$ is calculated to be 2.42 $\mu\Omega$ cm and the amount of transformation is only 3.3% after 480 min at 773 K. Under these conditions, i.e. $Y \ll 1$ Equation 4 is reduced to

$$Y = k\,t^n. \tag{5}$$

Substituting $Y$ from Equation 3

$$\Delta\rho = \Delta\rho_\infty\,k\,t^n. \tag{6}$$

Plots of log $\Delta\rho$ against log $t$ are shown in Fig. 8 for the six annealing temperautes below 848 K. The values of $n$ are between 0.67 and 0.72. At the lowest annealing temperature of 698 K the value of $n$ seems to change from 0.67 to 0.59 with increasing time. Thus the value of $n$ is close to 2/3 during the early stages of annealing at all temperatures below 848 K except at the lowest temperatures of 698 K.

The electron microscopic investigations show that at 848 K after only 97 min flat needles of $Al_6$Mn precipitate are present. Similar precipitates are apparent at 823 K after 300 and 1500 min. At 773 K flat needles of $G_2$-phase appear after 680 min. When the aging time is increased to 5790 min flat needles of $Al_6$Mn and more flat needles of $G_2$-phase were observed. At 723 K the precipitates which form on dislocations (Fig. 7) also appear to be elongated and when the annealing time is increased to 8760 min, they give rise to flat needles of $G_2$-phase. Thus during the early stages of annealing flat needle-like precipitates appear at all temperatures from 848 to 723 K, although they are $Al_6$Mn at $\geqslant 773$ K and $G_2$ at $\leqslant 773$ K. This is consistent with the same value of $n$ of 2/3 for all annealing temperatures for shorter annealing times.

The number of precipitate particles found at all temperatures and times was very low and the
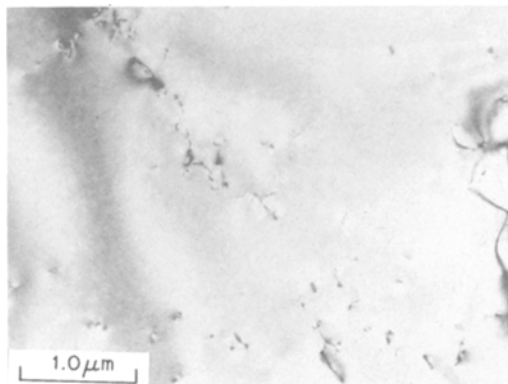


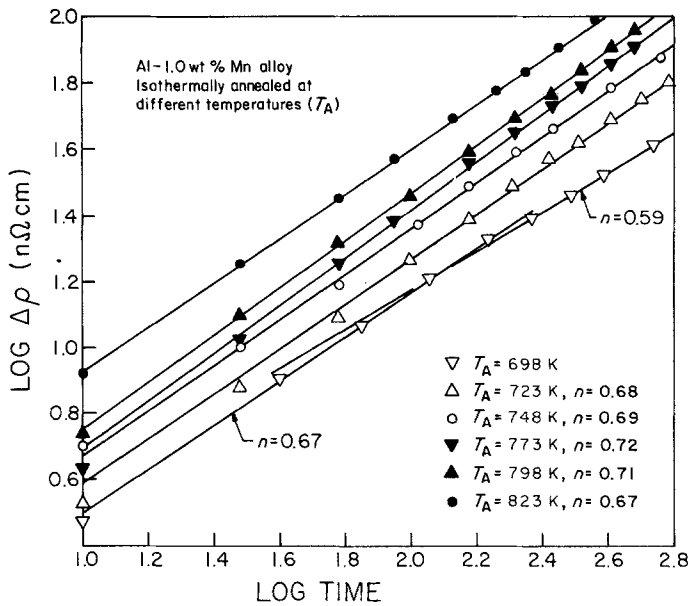Figure 7 Structure of a specimen aged for 775 min at 723 K.

*Figure 8* Log–log plot of $\Delta\rho$ against time for shorter annealing periods at various temperatures.

The plot contains:

Al–1.0 wt % Mn alloy
Isothermally annealed at
different temperatures ($T_A$)

$n = 0.59$
$n = 0.67$

| | |
|---|---|
| $\triangledown$ | $T_A = 698$ K |
| $\triangle$ | $T_A = 723$ K, $n = 0.68$ |
| $\circ$ | $T_A = 748$ K, $n = 0.69$ |
| $\blacktriangledown$ | $T_A = 773$ K, $n = 0.72$ |
| $\blacktriangle$ | $T_A = 798$ K, $n = 0.71$ |
| $\bullet$ | $T_A = 823$ K, $n = 0.67$ |

particles were well separated. This suggests that the nucleation rates of all the precipitates were low. Therefore, heterogenous nucleation on structural inhomogeneities like dislocations is the most likely precipitation mechanism. Fig. 7 shows that the precipitates do form on dislocations. This mode of precipitation is likely to be more predominant at higher temperatures because of the reduced driving force due to decreasing supersaturation. Ham [18] has shown that nucleation and growth of precipitates on dislocations can yield a value of 2/3 for $n$ in the early stages of precipitation. The same value of $n$ is observed in this investigation at all the annealing temperatures in the early stages.

As the temperature decreases, the driving force for precipitation increases and simultaneously the rate of nucleation also increases. As the annealing time increases, nearly isometric plates of G-phase appear. The G-phase was observed only after 6000 min of aging at 698 K and after 5790 min at 773 K. The G-phase has a regular well-defined shape, sharp boundaries with the matrix, and seems to possess a crystallographic relationship with the matrix, Nes *et al.* [5] observed interfacial dislocations around the G-phase concluding it to be semi-coherent with the aluminium matrix. Thus, both isometric semi-coherent plates of G and needles of $G_2$ appear at low temperatures after prolonged annealing.

When the annealing time is increased at 848 K, isometric thin plates of $Al_6Mn$ begin to appear. Even at 773 K such plates were observed on longer annealing times. These plates have a well-defined isometric shape and many of them seem to have a definite crystallographic relationship with the matrix. Therefore, they must have nucleated and grown along with flat needles at longer annealing times (Fig. 4). The value of the coefficient $n$ is found for longer annealing times at 848 K to be one. A value close to 1.0 has also been reported by other investigators near 848 K after longer annealing periods [2–4]. It may be noted that growth of the plates along their lengths and widths by normal diffusion can lead to a value of one for $n$ [17].

In this alloy system a sequence for the precipitation of various phases was not observed and all the phases seem to precipitate simultaneously. It is unusual to find metastable and stable phases coexisting in the same specimen. However, in Al–1.0 wt% Mn alloy, the rate of nucleation of all the phases is very low, so that only a few, well-separated precipitates form and their diffusion fields do not overlap. Therefore, they do not influence others' growth. However, still longer annealing times may be required for the transformation of the metastable phases to $Al_6Mn$.

## 5. Conclusions

(1) The precipitation kinetics in Al–1.0 wt% Mn alloy can be expressed by $Y = 1 - \exp(-kt^n)$ where the time exponent $n$ varies with temperature and time. The value of $n$ was found to be 2/3 in the initial stages at all the annealing temperatures investigated. However, at 848 K, the value of

$n$ increases to 1.0 on longer annealing times and at 698 K the value decreases to 0.59.

(2) Flat, thin needles of the equilibrium phase $Al_6Mn$ were observed above 773 K. However, at longer annealing times thin isometric plates of $Al_6Mn$ were also observed. Flat, thin needles of $G_2$ were observed at and below 773 K, but thin plates of G-phase were observed only on longer annealing times at or below 773 K.

(3) Precipitates formed during early stages of annealing were found on dislocations.

(4) All the precipitates had regular, well-defined shapes and the majority appeared to have a crystallographic relationship with the matrix. The observed precipitates and their morphologies are consistent with the time exponent of the kinetic equation.

## Acknowledgements

## References

1. F. A. SHUNK. "Constitution of Binary Alloys", Second Supplement, (McGraw Hill, New York, 1969) p. 29.
2. D. OELSCHLAGEL, O. KAWANO and O. IZUMI, *J. Japan Inst. Light Metals* **20** (1970) 531.
3. D. B. GOEL, P. FURRER and H. WARLIMONT, *Aluminium* **50** (1974) 511.
4. A. FERRARI, P. FIORINI and F. GATTO, *Alumino* **35** (1966) 223.
5. E. NES, S. E. NAESS and R. HOIER, *Z. Metallkde.* **63** (1972) 248.
6. R. HOIER, S. E. NAESS and E. NES, *ibid.* **64** (1973) 640.
7. W. B. PEARSON, "Handbook of Lattice Spacings and Structure of Metals", (Pergamon Press, Oxford, 1967).
8. K. LITTLE, G. V. RAYNOR and W. HUME-ROTHERY, *J. Inst. Metals* **73** (1946) 83.
9. G. MARCHAND, *ibid.* **73** (1946) 747.
10. J. ADAM and J. B. RICH, *Acta Cryst.* **7** (1954) 813.
11. O. IZUMI, O. KAWANO and D. OELSCHLAGER, Septieme Congrés Int. de Microscopie Electronique, Grenoble, **2** (Societe Francaise de Microscopie Electronique, Paris, 1970) 535.
12. K. ROBINSON, *Phil. Mag.* **43** (1952) 775.
13. D. P. LAHIRI, A. K. JENA and T. R. RAMACHANDRAM, *J. Mater. Sci.* **10** (1975) 1458.
14. T. FEDERIGHI, "Lattice Defects in Quenched Metals", (Academic Press, London and New York, 1965) p. 217.
15. F. R. FICKETT, *Cryogenics* **11** (1971) 349.
16. F. J. KEDVES, L. GERGELY, M. HORDOS and E. KOVACSETENYI, *Phus. Stat. Solidi (a)* **13** (1972) 685.
17. J. W. CHRISTIAN, "The Theory of Phase Transformations in Metals and Alloys", (Pergamon Press, Oxford, 1965) p. 481.
18. F. S. HAM, *J. Appl. Phys.* **30** (1959) 915.